

Evidence for large electric polarization from collinear magnetism in TmMnO_3

V. Yu. Pomjakushin¹, M. Kenzelmann^{1,2}, A. Dönni³, A. B. Harris⁴, T. Nakajima⁵, S. Mitsuda⁵, M. Tachibana⁶, L. Keller¹, J. Mesot¹, H. Kitazawa³, E. Takayama-Muromachi⁶

(1) *Laboratory for Neutron Scattering,*

ETH Zürich & Paul Scherrer Institute, CH-5232 Villigen, Switzerland

(2) *Laboratory for Solid State Physics,*

ETH Zürich, CH-8093 Zürich, Switzerland

(3) *National Institute for Materials Science (NIMS),*

1-2-1 Sengen, Tsukuba, Ibaraki 305-0047, Japan

(4) *Department of Physics and Astronomy,*

University of Pennsylvania, Philadelphia, Pennsylvania 19104, USA

(5) *Department of Physics, Faculty of Science,*

Tokyo University of Science, 1-3 Kagurazaka,

Shinjuku-ku, Tokyo 162-8601, Japan

(6) *National Institute for Materials Science (NIMS),*

1-1 Namiki, Tsukuba, Ibaraki 305-0044, Japan

(Dated: November 1, 2021)

Abstract

There has been tremendous research activity in the field of magneto-electric (ME) multiferroics after Kimura *et al.* [1] showed that antiferromagnetic and ferroelectric order coexist in orthorhombically distorted perovskite TbMnO_3 and are strongly coupled. It is now generally accepted that ferroelectricity in TbMnO_3 is induced by magnetic long range order that breaks the symmetry of the crystal and creates a polar axis [2]. One remaining key question is whether magnetic order can induce ferroelectric polarization that is as large as that of technologically useful materials. We show that ferroelectricity in orthorhombic (o) TmMnO_3 is induced by collinear magnetic order, and that the lower limit for its electric polarization is larger than in previously investigated orthorhombic heavy rare-earth manganites. The temperature dependence of the lattice constants provides further evidence of large spin-lattice coupling effects. Our experiments suggest that the ferroelectric polarization in the orthorhombic perovskites with commensurate magnetic ground states could pass the $1\mu\text{C}/\text{cm}^2$ threshold, as suggested by theory [3, 4].

PACS numbers: 75.80.+q, 75.25.+z, 77.80.-e

Multiferroic materials are defined as materials with more than one switchable spontaneous order parameter such as ferromagnetism and ferroelectricity. It has become custom to include materials with coexisting spontaneous antiferromagnetic and ferroelectric order in the class of ME multiferroics. One can distinguish two major classes of ME multiferroics: those where the onset of ferroelectricity is unrelated to magnetic order, and those where ferroelectricity is induced by magnetic order. Hexagonal YMnO₃ is an example of a multiferroic material where the onset of ferroelectricity is completely unrelated to the onset of magnetism, and probably arises from geometrical effects [5]. Orthorhombic TbMnO₃ is an example of a multiferroic material where ferroelectricity arises from magnetic spiral order [1, 2, 6]. Ferroelectricity from magnetic order is related to competing magnetic interactions, whose competition at low temperatures is reduced through small lattice distortions that result in switchable electric polarization.

Magnetically induced ferroelectricity has been observed for structurally very different materials, most notably in rare-earth (R) manganites RMn₂O₅ [7, 8], the kagome staircase magnet Ni₃V₂O₈ [9], and the triangular lattice antiferromagnet RbFe(MoO₄)₂ [10]. This suggests that the mechanism to obtain ferroelectricity from magnetic order is quite general and should be present in many materials. In all these materials, ferroelectric polarization arises, at least partly, from incommensurate spiral magnetic structures that lead to polar structures. The ME interaction in these materials is believed to be mediated by spin-orbit interactions, and so the ferroelectric polarization is relatively small.

Much larger ferroelectric polarizations were predicted for materials where ferroelectricity arises from *collinear* magnetic order [3, 4]. In such materials, ME coupling may be mediated by the symmetric exchange which is larger than spin-orbit related interactions. An example is orthorhombic (o) HoMnO₃ where ferroelectricity arises from commensurate, collinear magnetic order [11, 12]. However, the ferroelectric polarization in o-HoMnO₃ was observed to be much smaller than predicted [4], and arises partly from rare-earth magnetic order [11]. Here, we present the case of o-TmMnO₃ for which we observed a ferroelectric polarization that arises from collinear Mn³⁺ magnetic order, and that is at least 15 times larger than observed for o-HoMnO₃. We provide evidence for spin-lattice coupling effects that are larger than in other magnetically-induced ferroelectrics.

TmMnO₃ crystallizes in the space group Pnma and has room-temperature lattice parameters $a = 5.809 \text{ \AA}$, $b = 7.318 \text{ \AA}$ and $c = 5.228 \text{ \AA}$. A projection of the crystal structure

onto the ac plane is shown in Fig. 1. The unit cell contains four Mn^{3+} ions, located at $\mathbf{r}_1 = (0, 0, 0.5)$, $\mathbf{r}_2 = (0.5, 0.5, 0)$, $\mathbf{r}_3 = (0.5, 0, 0)$, and $\mathbf{r}_4 = (0, 0.5, 0.5)$. The large rotation of the oxygen octahedra around the Mn^{3+} ions is expected to result in appreciable antiferromagnetic superexchange interactions along the a axis through pairs of oxygen anions [13] that compete with the ferromagnetic interactions in the ac plane.

Our neutron diffraction data, shown in Fig. 2, feature new Bragg peaks below $T_N^{\text{Mn}} = 42$ K and demonstrate that TmMnO_3 adopts magnetic order below T_N^{Mn} . The ordering wave-vector is $\mathbf{Q} = (q, 0, 0)$ where q is the modulation wave-number along the a axis. The temperature dependence of the magnetic neutron Bragg peaks indicates a second-order transition at T_N^{Mn} , as shown in Fig. 3, and an anomaly at $T_C = 32$ K indicates a further transition. These two transitions coincide with peaks in the temperature dependence of the specific heat [14]. The temperature dependence of the magnetic peaks close to $\mathbf{Q} = (0.5, 1, 0)$ (Fig. 3c) shows that the magnetic structure is incommensurate for $T_C < T < T_N^{\text{Mn}}$ and commensurate for $T < T_C$. In the incommensurate phase, the ordering wave-vector is $\mathbf{Q} = (q, 0, 0)$ with $0.45 < q \leq 0.5$.

The incommensurate magnetic order is described by one single order parameter, described in more detail in Methods, at $T = 35$ K with an amplitude only on the Mn^{3+} ions given by $\mathbf{m}_{\text{IC}}^1 = [2.98(2), 0.0(5), \exp(i\phi) 0.95(3)] \mu_B$, where ϕ is the relative phase between the a and c - components. Although we cannot experimentally determine ϕ , it can be shown that because of the inversion center of the paramagnetic phase, $\exp(i\phi) = \pm 1$ [15]. No magnetic order was detected on the Tm^{3+} ions in the incommensurate phase. Thus the spins are amplitude modulated with moments collinear at an angle to the a axis, as shown in Fig. 1a. This is slightly different from the incommensurate order in HoMnO_3 that is collinear [12].

The commensurate structure at $T = 2$ K is described by two-dimensional order parameter as specified in Methods. The magnetic order is a E-type magnetic structure shown in Fig. 1b-c, with $3.75(3)\mu_B$ magnetic moment ordered on the Mn^{3+} sites along the a axis. The E-type magnetic structure can have two independent basis vector for the moments along the a -axis: $E_1 = (1, 1, -1, -1)$ and $E_2 = (1, -1, 1, -1)$ in the order of the Mn^{3+} ion as defined above - identical to the low-temperature Mn^{3+} order in HoMnO_3 [12]. In addition, we found that Tm^{3+} has an ordered moment of $1.22(5)\mu_B$ pointing along the c axis at 2 K. Because the Tm^{3+} moments are allowed only along the b -axis if they were magnetically polarized by the Mn^{3+} order, this implies that the Tm^{3+} undergo independent spontaneous magnetic order,

as indicated by a peak in the specific heat at around $T_N^{\text{Tm}} = 4$ K [14].

Fig. 4a shows that TmMnO_3 has a macroscopic response to the onset of magnetic long-range order and develops spontaneous electric polarization P below 32 K, demonstrating that o-TmMnO_3 has a multiferroic ground state. The observed value of P for a powder sample, $P = 1500 \mu\text{C}/\text{m}^2$, is more than 15 times larger than that of o-HoMnO_3 [11]. The value of P for a powder sample is half the intrinsic value for a single crystal, namely $P_0 = 0.3 \mu\text{C}/\text{cm}^2$. Since we have not observed the saturation of $P(E)$, as shown in the inset of Fig. 4a, P_0 may be substantially higher and our observation is a lower limit of the intrinsic polarization. The reported electric polarization in o-HoMnO_3 was much smaller, so our results suggest that sample quality or the details of the crystal structure are decisive for the size of the electric polarization in the orthorhombic rare earth manganites. The experimentally observed polarization (which is merely a lower limit for the intrinsic electric polarization) is the highest observed value for magnetically induced ferroelectricity to date, and is of the same order as the values $P_0 = 0.5 - 12 \mu\text{C}/\text{cm}^2$ [3] and $6 \mu\text{C}/\text{cm}^2$ [4] predicted (but not observed) for HoMnO_3 . This provides strong experimental evidence that the theoretically predicted mechanism of symmetric exchange, although not universal to all o-RMnO_3 systems, does apply in the case of TmMnO_3 and can give rise to magnetically-induced ferroelectricity that is large enough for applications.

From the magnetic structures shown in Fig. 1 we propose a likely scenario for the magnetic exchange interactions in TmMnO_3 . These structures suggest that the interactions between second neighbors are ferromagnetic along the c axis and are antiferromagnetic along the a and b axes. In the commensurate phase (for $T < T_C$) the distortion of the nearest neighbor bonds is such that the straighter bonds have an interaction that is less ferromagnetic (or more antiferromagnetic) than the bent bonds, thus removing the frustration that would occur in the absence of the distortion. For $T_C < T$, when the bonds are undistorted, the frustration is removed by the incommensurate structure of Fig. 1a.

The magnetic order is never strictly long-range, because magnetic Bragg peaks were found to be always wider than the resolution-limited nuclear Bragg peaks. Fig. 3d shows that the magnetic correlation length does never exceed 600 nm, and most probably arises from ferroelectric domains. Picozzi et. al. [4] showed that ferroelectric polarization in HoMnO_3 is generated mostly through movements of the Mn^{3+} and O^{2-} positions, so the magnetic structure E_1 and E_2 (shown in Fig. 1) favor opposite ferroelectric polarization,

as can be seen from the phenomenological formula $P_0 \propto (E_1^2 - E_2^2)$. Thus the magnetic structure E_1 and E_2 must be separated by a magnetic domain walls, limiting the magnetic correlation length to the size of the ferroelectric domains. Our measurements thus suggest that the magnetic domains can be controlled by electric fields.

The temperature dependence of the real part of the dielectric susceptibility, shown in Fig. 4c provides evidence for the ferroelectric transition at $T_C = 32$ K, in agreement with the pyroelectric measurements. The imaginary part of the dielectric constant, shown in Fig. 4d, shows a two-peak feature as a function of temperature, and relatively high values between $T_N^{\text{Tm}} = 4$ K and $T_C = 32$ K that suggest substantial energy dissipation. The energy dissipation in this temperature range may result from slow switching behavior associated with the magnetically polarized Tm^{3+} magnetic moments that are only loosely coupled to the rapidly switching Mn^{3+} . Below $T_N^{\text{Tm}} = 4$ K, the Tm^{3+} moments are spontaneously ordered and therefore not directly connected to the electric order, so that dielectric constant shows no dissipation, as shown in Fig. 4d. This scenario is also consistent with a flattening off of the electric polarization stops below $T_N^{\text{Tm}} = 4$ K, suggesting that the Tm^{3+} order competes with the Mn^{3+} order and thereby limits the size of the electric polarization.

Independent evidence for strong coupling between the chemical and magnetic lattice is also seen in the temperature dependence of the lattice constants, shown in Fig. 5. These spin-lattice effects are larger than in any other heavy rare-earth o-RMnO₃, suggesting that the magnetic order has a stronger effect on the chemical lattice of o-TmMnO₃ than in other heavy rare-earth manganites. Our results can be understood phenomenologically as follows. Because the incommensurate magnetic order is described by only a single one-dimensional order parameter, there can be no magnetically-induced ferroelectricity in accordance with our experiment [15]. In the commensurate phase the ME interaction is of the form given in Ref. 3. However, the fourth order terms in the magnetic free energy cause either $E_1 \cdot E_2 = 0$ or $|E_1| = |E_2|$, depending on the sign of the fourth order spin anisotropy[16]. Thus the higher order ME interaction in Ref. 3 is generally inoperative and the polarization is restricted to lie along the c axis with magnitude $P_c \propto (E_1^2 - E_2^2)$, where $E_1 E_2 = 0$ is selected. The temperature dependence of P is only qualitatively consistent with this, possibly because the results are somewhat modified by the sample not being a single crystal.

In summary, we have shown that TmMnO₃ has a magnetically-induced electric polarization that is substantially higher than in any other heavy rare-earth manganites with

commensurate magnetic order. We observed anomalies in the temperature dependence of the lattice constants at the magnetic phase transitions that are evidence for strong coupling effects between the chemical and magnetic lattices. Theoretical calculations have predicted a large spontaneous electric polarization in HoMnO_3 , at variance with current experimental results [4]. Since we have found such a large polarization in TmMnO_3 , it is of great interest to have such calculations made for this system and hopefully to understand the difference between HoMnO_3 and TmMnO_3 .

We acknowledge valuable discussions with R. A. Cowley, N. A. Spaldin, and D. Khomskii. This work was supported by the Swiss NSF (Contract No. PP002-102831). This work is based on experiments performed at the Swiss spallation neutron source SINQ, Paul Scherrer Institute.

Methods

Polycrystalline samples of perovskite TmMnO_3 were prepared under high pressure as described in Ref. 14. Neutron powder diffraction measurements were performed on a large amount (5.4 g) of TmMnO_3 sample using the HRPT and DMC diffractometers at the Paul Scherrer Institute, and incident neutrons with a wave-length of 1.89 Å and 4.5 Å, respectively. The magnetic structures were determined using the Fullprof Suite [17]. The size of the magnetic moments have been determined by comparing the strength of magnetic and nuclear intensities. No texture effects were observed during the analysis.

The ferroelectric polarization was determined using a 0.4 mm thin hardened pellet of polycrystalline TmMnO_3 covered with an area $3.12 \cdot 10^{-6} \text{ m}^2$ of silver epoxy. The sample was cooled from 50 K to 2 K in poling electric fields of up to $E = 3750 \text{ kV/m}$, after which the electric field was reduced to zero and the sample was allowed to discharge for 5 minutes. After the discharge at 2 K the residual current was reduced to 10^{-14} A , which suggests that trapped charges did not affect the pyroelectric measurement. Then the sample was heated at different constant rates between 0.85 and 4.86 K/min and the pyroelectric current was measured using a Keithley 6517A electrometer, resulting in nearly identical estimates of the ferroelectric polarization. Pyroelectric measurements at different ramping speeds and a stop-and-go ramp result in a nearly identical temperature dependent electric polarization, showing

the thermal excitation of trapped charges does not affect the pyroelectric measurements. These measurements therefore allow the determination of the lower limit of the electric polarization. Real and imaginary part of the dielectric constant were measured using a Agilent E4980A LCR meter, making sure that the Maxwell-Wagner effect does not affect the measurements. The magnetic susceptibility was measured in an external field $H = 100$ Oe on a small (5.9mg) powder sample using a Quantum Design SQUID magnetometer.

The incommensurate magnetic structure belongs to irreducible representation Γ_{IC}^3 , where the superscript corresponds to Kovalev's notation [18], and is defined by the following characters: $\chi(I) = 1$, $\chi(2_a) = -\alpha$, $\chi(m_{ab}) = -\alpha$ and $\chi(m_{ac}) = 1$, with $\alpha = \exp(i\pi q)$. Here 2_a is a two-fold screw axis rotation, while m_{ab} and m_{ac} are ab/ac -mirror planes followed by a (0.5, 0, 0.5) or (0, 0.5, 0) lattice translation, respectively. The commensurate structure at $T = 2$ K is described by the two-dimensional irreducible representation Γ_{C}^1 according to Kovalev's notation and defined by the following non-zero characters: $\chi(I) = 2$ and $\chi(m_{ac}) = -2$.

-
- [1] Kimura, T. *et al.* Magnetic control of ferroelectric polarization. *Nature* **426**, 55 (2003).
 - [2] Kenzelmann, M. *et al.* Magnetic inversion symmetry breaking and ferroelectricity in TbMnO₃. *Phys. Rev. Lett.* **95**, 087206 (2005).
 - [3] Sergienko, I. A., Sen, C. & Dagotto, E. Ferroelectricity in the magnetic e-phase of orthorhombic perovskites. *Phys. Rev. Lett.* **97**, 227204 (2006).
 - [4] Picozzi, S. *et al.* Dual nature of improper ferroelectricity in a magnetoelectric multiferroic. *Phys. Rev. Lett.* **99**, 227201 (2007).
 - [5] Van Aken, B. B., Palstra, T. T. M., Filippetti, A. & Spaldin, N. A. The origin of ferroelectricity in magnetoelectric YMnO₃. *Nature Materials* **3** 164 (2004).
 - [6] Mostovoy, M. Ferroelectricity in spiral magnets. *Phys. Rev. Lett.* **96**, 067601 (2006).
 - [7] Hur, N. *et al.* Electric polarization reversal and memory in a multiferroic material induced by magnetic fields. *Nature* **429**, 392 (2004).
 - [8] Harris, A. B. , Aharony, A. & Entin-Wohlman, O. Order parameters and phase diagrams of multiferroics. *J. Phys. Condens. Mat.* **20**, 434202 (2008).
 - [9] Lawes, G. *et al.* Ferroelectricity through Magnetic Inversion Symmetry Breaking on a Kagome

- Staircase. *Phys. Rev. Lett.* **95**, 087205 (2005).
- [10] Kenzelmann, M. *et al.* Direct transition from a disordered phase to an incommensurate multiferroic on a triangular lattice. *Phys. Rev. Lett.* **98**, 267205 (2007).
- [11] Lorenz, B., Wang, Y. Q., Chu, C. W., Ferroelectricity in perovskite HoMnO_3 and YMnO_3 . *Phys. Rev. B* **76**, 104405 (2007).
- [12] Munoz, A. *et al.* Complex magnetism and magnetic structures of the metastable HoMnO_3 perovskite. *Inorg. Chem.* **40**, 1020 (2001).
- [13] Kimura, T., Ishihara, S., Shintani, H., Arima, T., Takahashi, K. T., Ishizaka, K. & Tokura, Y. Distorted perovskite with e_g^1 configuration as a frustrated spin system. *Phys. Rev. B* **68**, 060403(R) (2003).
- [14] Tachibana, M., Shimoyama, T., Kawaji, H., Atake, T. & Takayama-Muromachi, E. Jahn-Teller distortion and magnetic transitions in perovskite RMnO_3 (R=Ho, Er, Tm, Yb, and Lu). *Phys. Rev. B* **75**, 144425 (2007).
- [15] Harris, A. B. Landau analysis of the symmetry of the magnetic structure and magnetoelectric interaction in multiferroics. *Phys. Rev. B* **76**, 054447 (2007).
- [16] Harris, A. B., Aharony, A. & Entin-Wohlman, O. Order parameters and phase diagram of multiferroic RMn_2O_5 . *Phys. Rev. Lett.* **100** 217202 (2008).
- [17] J. Rodriguez-Carvajal, *The FullProf Suite*, <http://www.ill.eu/sites/fullprof/>
- [18] Kovalev, O. V., *Representations of the Crystallographic Space Groups*, edited by H. T. Stokes & D M. Hatch, Gordon and Breach, London (1993).

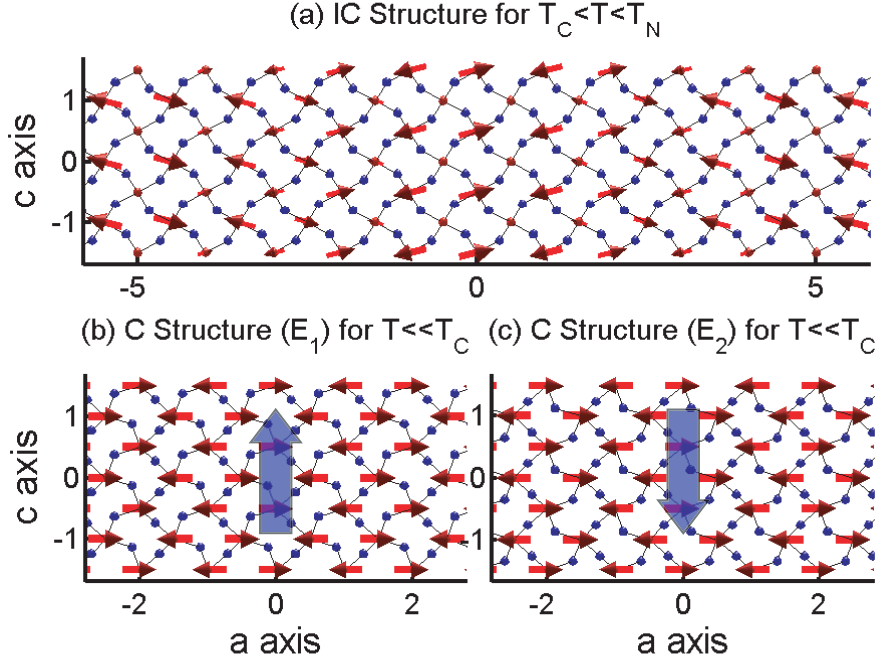


FIG. 1: Chemical structure of TmMnO_3 , showing Mn^{3+} in red and O^{2-} in blue. (a) Incommensurate amplitude-modulated Mn^{3+} spin order in the paraelectric phase for $32 \text{ K} < T < 40 \text{ K}$. (b-c) Commensurate Mn^{3+} spin order of E_1 and E_2 type, respectively, in the ferroelectric phase for $T \ll 32 \text{ K}$. The large arrows show the direction of the spontaneous polarization along the c axis that arises from a movement of the Mn^{3+} and O^{2-} positions (shown here schematically) to adjust the Mn-O-Mn angle for parallel and antiparallel nearest-neighbor alignment, thereby lowering symmetry through the creation of a polar axis. (a-c) The moments in the neighboring planes are oriented in the opposite direction.

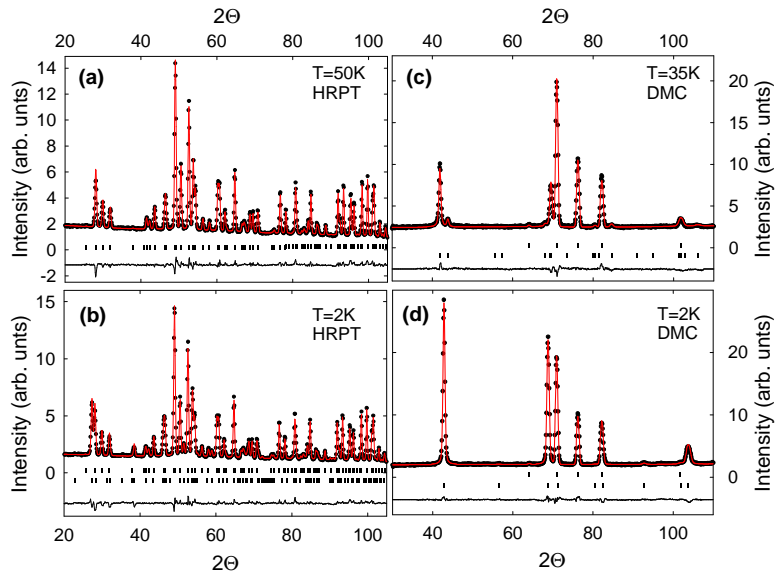


FIG. 2: Part of the neutron scattering patterns measured using HRPT, as a function of scattering angle 2θ at (a) $T = 50$ K showing only nuclear scattering, and (b) $T = 2$ K showing additionally magnetic scattering. (c-d) Bragg peak powder patterns measured using DMC at $T = 35$ K and $T = 2$ K. (a-d) The vertical bars indicate magnetic and nuclear (upper row) Bragg peaks. The bottom solid line indicates the difference between the experiment and the model.

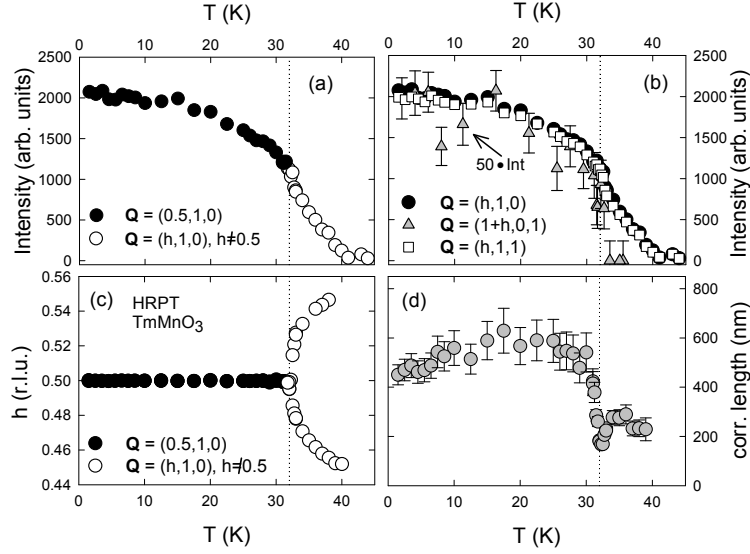


FIG. 3: (a) Temperature dependence of the magnetic Bragg peak intensity at $\mathbf{Q} = (0.5, 1, 0)$ in the commensurate phase, or the added intensities at the $\mathbf{Q} = (q, 1, 0)$ and $\mathbf{Q} = (1 - q, 1, 0)$ Bragg peak positions for $0.45 < q \leq 0.5$. (b) Comparison of the temperature dependence of different magnetic Bragg peaks, showing that they have the same temperature dependence in the commensurate phase. The $\mathbf{Q} = (1.5, 0, 1)$ Bragg peak is only present in the commensurate phase, and is evidence of the ordering of Tm^{3+} magnetic moments. (c) Temperature dependence of the a-component, h , of the magnetic Bragg peak $\mathbf{Q} = (h, 1, 0)$, where $h = q$ or $h = 1 - q$. (d) Temperature dependence of the magnetic correlation length as deduced from the width of the magnetic Bragg peaks.

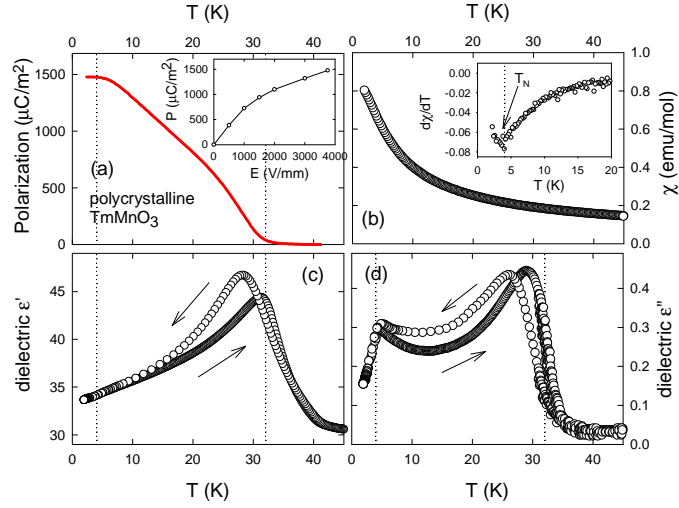


FIG. 4: (a) Electric polarization of a pressed powder sample of o -TmMnO₃ as a function of temperature, determined using pyroelectric measurements after cooling an electrically poled sample. Inset: Electric polarization at $T = 2$ K as a function of poling electric field with which the sample was cooled. (b) Magnetic susceptibility as a function of temperature measured on cooling. Inset: Temperature derivative of the magnetic susceptibility indicating the onset of spontaneous Tm³⁺ magnetic order at $T_N^{\text{Tm}} = 4$ K. (c) Real and (d) imaginary part of the dielectric susceptibility as a function of temperature, measured at a frequency of $f = 100$ kHz.

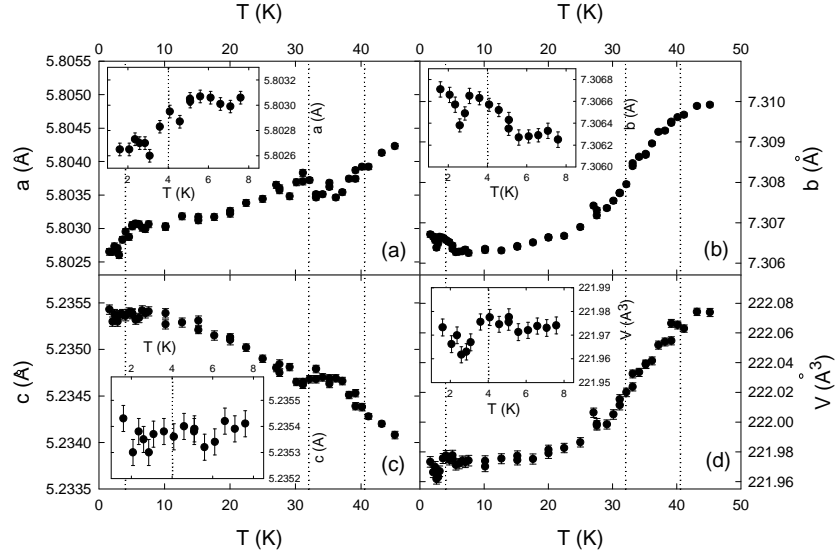


FIG. 5: Temperature dependence of the lattice constants for $T < 50$ K. The insets show additional transitions below 4 K. The vertical dotted lines at T_N^{Mn} and T_C indicate magnetic transitions, while the vertical dotted line at $T_N^{\text{Tm}} = 4$ K indicates the onset of spontaneous Tm^{3+} magnetic order.